

Measurement of Hemoglobin Oxygenation Parameters in Arterial Occlusion and Physical Exertion

D. A. Buyanov,^{1,2} P. V. Shalaev,² S. V. Zabodaev,³ P. A. Monakhova,^{1,4} D. D. Stavtsev,^{1,5,*}
A. N. Konovalov,⁶ and A. Yu. Gerasimenko^{1,5}

Near-infrared spectroscopy is widely used for the non-invasive measurement of hemoglobin oxygenation in biological tissues. Here we report experimental studies on the measurement of oxygenation parameters during arterial occlusion and physical exertion using the NIRS4 hardware/software system and a previously developed algorithm based on a modified Bouguer–Lambert–Beer law. The dynamics of changes in hemoglobin oxygenation parameters during arterial occlusion and physical exertion of the quadriceps femoris and biceps brachii muscles are demonstrated. The measurement results demonstrate that the NIRS4 system, together with the present algorithm, can be used to analyze the dynamics of hemoglobin oxygenation.

Introduction

Near infrared spectroscopy has become widespread as a noninvasive method for assessing the degree of oxygen saturation of hemoglobin in biological tissues, including skeletal muscles [1, 2]. This method is based on measuring the attenuation of light in the near infrared range (700–1000 nm) due to absorption by chromophores in tissues [3]. This effect can be described by the Bouguer–Lambert–Beer law, whereby the attenuation of light is directly proportional to the product of the chromophore concentration and the optical path length. In highly scattering media such as biological tissues, the effects of multiple scattering cause the physical path length of a photon to be greater than the distance between the source

and the receiver. The effect of scattering is described by the modified Bouguer–Lambert–Beer law.

One of the main light-absorbing chromophores in biological tissues is hemoglobin, which consists of two main fractions: oxygenated (HbO₂) and deoxygenated (Hb). Each fraction has its own optical absorption characteristics [4], which can be measured using near-infrared spectroscopy. This method can be used to determine blood oxyhemoglobin saturation (StO₂) and the absolute and relative concentrations of the hemoglobin fractions.

The aim of the present work was to carry out experimental testing of a previously developed algorithm for calculating changes in the oxygenation index based on the modified Bouguer–Lambert–Beer law.

Materials and Methods

Scattered radiation was detected using a NIRS4 hardware/software system, which included a three-frequency LED radiation source with wavelengths of 770, 810, and 850 nm, located in the center, and four radiation receivers mounted on flexible petals around the perimeter at equal distances from the emitter. The radiation source formed light pulses at these three wavelengths in sequence. The wavelengths selected correspond to the characteristic absorption peaks of HbO₂, Hb, and total hemoglobin (Hb_t) respectively.

An algorithm for measuring the absolute and relative concentrations of oxygenated and deoxygenated hemoglobin based on the modified Bouguer–Lambert–Beer law using

¹Institute of Biomedical Systems, National Research University of Electronic Technology, Zelenograd, Moscow;
E-mail: stavtsev.dmitry@gmail.com

²Department of Registration and Certification of Medical Devices, OOO Medical Computer Systems, Zelenograd, Moscow.

³OOO Medical Computer Systems, Zelenograd, Moscow.

⁴Development Department, Aivok, Zelenograd, Moscow.

⁵Institute of Bionic Technologies and Engineering, I. M. Sechenov First Moscow State Medical University, Russian Ministry of Health, Moscow.

⁶Third Neurosurgery Department, N. N. Burdenko National Medical Research Center for Neurosurgery, Russian Ministry of Health, Moscow.

*To whom correspondence should be addressed.

the NIRS4 system was previously proposed in [5]. This original empirical model, which establishes the relationship between the absolute concentrations of oxygenated and deoxygenated hemoglobin on the one hand and the intensity of radiation detected by the device on the other, is based on preliminary calibration of the device using phantoms of scattering biological objects with known optical properties. The model takes account of the light absorption by all biological substances present in living tissue, in addition to the two hemoglobin fractions. Within the framework of this model, the absolute oxygenated and deoxygenated hemoglobin concentrations were determined as [5]

$$\left\{ \begin{array}{l} C_{\text{Hb}} = \frac{1}{r_{\text{SD}}} \frac{1}{DPF} \\ \times \frac{\varepsilon_{\text{HbO}_2}^{770} \left(-\ln \frac{I^{850}}{I_0^{850}} - \tilde{G}^{850} \right) - \left(-\ln \frac{I^{770}}{I_0^{770}} - \tilde{G}^{770} \right) \varepsilon_{\text{HbO}_2}^{850}}{\varepsilon_{\text{HbO}_2}^{770} \varepsilon_{\text{Hb}}^{850} - \varepsilon_{\text{Hb}}^{770} \varepsilon_{\text{HbO}_2}^{850}} ; \\ C_{\text{HbO}_2} = \frac{1}{r_{\text{SD}}} \frac{1}{DPF} \frac{\left(-\ln \frac{I^{770}}{I_0^{770}} - \tilde{G}^{770} \right) - \varepsilon_{\text{Hb}}^{770} C_{\text{Hb}}}{\varepsilon_{\text{HbO}_2}^{770}} , \end{array} \right. \quad (1)$$

where r_{SD} is the distance between the radiation source and the receiver; DPF is the differential path length factor, which takes the increase in the length of the photon migration path due to scattering into account; $\varepsilon_{\text{HbO}_2}^{770}$, $\varepsilon_{\text{Hb}}^{850}$, $\varepsilon_{\text{Hb}}^{770}$, and $\varepsilon_{\text{HbO}_2}^{850}$ are the absorption indexes at wavelengths of 770 and 850 nm of oxyhemoglobin and deoxyhemoglobin respectively; I^{770} , I^{850} , I_0^{770} , and I_0^{850} are the intensities of the detected and incident radiation at the corresponding wavelengths; \tilde{G}^{770} and \tilde{G}^{850} are the modified attenuation factors for radiation at the corresponding wavelengths.

When C_{Hb} and C_{HbO_2} are known, the functional saturation of blood oxyhemoglobin can be determined [6]:

$$\text{StO}_2 = \frac{C_{\text{HbO}_2}}{C_{\text{HbO}_2} + C_{\text{Hb}}} 100 \% . \quad (2)$$

Most approaches to analysis of the dynamics of changes in oxygenated and deoxygenated hemoglobin concentrations involve preliminary measurement of the baseline followed by experimental measurement of shifts relative to this baseline [7–11].

An expression was derived from Eq. (1) to determine the relative oxygenated and deoxygenated hemoglobin concentrations:

$$\left\{ \begin{array}{l} \Delta C_{\text{Hb}} = - \frac{1}{r_{\text{SD}} DPF} \frac{\varepsilon_{\text{HbO}_2}^{770} \ln \frac{I^{850}(t_1)}{I^{850}(t_0)} - \varepsilon_{\text{HbO}_2}^{850} \ln \frac{I^{770}(t_1)}{I^{770}(t_0)}}{\varepsilon_{\text{HbO}_2}^{770} \varepsilon_{\text{Hb}}^{850} - \varepsilon_{\text{Hb}}^{770} \varepsilon_{\text{HbO}_2}^{850}} ; \\ \Delta C_{\text{HbO}_2} = \frac{- \frac{1}{r_{\text{SD}} DPF} \ln \frac{I^{770}(t_1)}{I^{770}(t_0)} - \varepsilon_{\text{Hb}}^{770} \Delta C_{\text{Hb}}}{\varepsilon_{\text{HbO}_2}^{770}} , \end{array} \right. \quad (3)$$

where $I^{770}(t_0)$ and $I^{850}(t_0)$ are radiation intensity values measured at rest.

The algorithm used averaged values measured at the beginning of the experiment as $I^{770}(t_0)$ and $I^{850}(t_0)$ for measurement of relative oxygenated and deoxygenated hemoglobin concentrations.

Calculation of relative oxygenated and deoxygenated hemoglobin concentrations using Eq. (3) does not require knowledge of the intensity of the incident radiation I_0 or the attenuation factor G , which is an advantage of this approach.

A number of experiments were run to confirm the effectiveness of the algorithm by measuring hemoglobin oxygenation parameters in tissues during arterial occlusion and physical exertion.

The use of arterial occlusion has become widespread — this method is conventionally used as a standard approach for evaluating the performance of various methods and devices for spectroscopy in the near infrared range [8, 11]. For the present experiments, the NIRS4 system was attached to the inner aspect of the forearm. Measurements were initially taken at rest, after which the brachial artery was compressed using a sphygmomanometer cuff, in which pressure was maintained at a least 280 mmHg for 1–4 min. At the final stage, the pressure in the cuff was quickly released and measurements were continued for another 1–5 min.

Measurements of hemoglobin oxygenation parameters during exercise were made in two experiments. In the first, the device was attached to the quadriceps muscle of the thigh and measurements were made at rest; the subject then performed squats for 4.5 min, which was followed by taking measurements for a further 5 min. In the second experiment, the device was attached to the biceps brachii. Measurements were taken at rest, after which concentrated dumbbell lifts with a mass of 5 kg per biceps were performed for 2.5 min, which was followed by taking measurements for another 6 min.

Data from the device were saved using the LabRecorder program and then processed using the present algorithm. As small displacements of the instrument during experiment led to noise in the dataset, the initial data were first filtered with a median filter.

Results

The results of measurements of hemoglobin oxygenation parameters during arterial occlusion are shown in Fig. 1. Use of the present computation algorithm allowed the dynamics of the process to be analyzed. In particular, the results showed that after approximately 3.5 min of occlusion, the saturation value stopped decreasing and reached a plateau. This effect may be associated with a decrease in the oxygenated hemoglobin concentration to a minimum value [Fig. 1d shows that there was no sensor exposure during the experiment (1.2 units) or that the signal was too weak (0 units)].

Resumption of normal blood circulation was followed by a hypercompensation effect: the saturation value exceeded the initial value at rest, after which it began a gradual decrease to the normal level. Moreover, the return to the normal level occurred with characteristic fluctuations.

Measurement results at the thigh and forearm are shown in Fig. 2. The dynamics of changes in hemoglobin oxygenation parameters during physical exertion were similar to the dynamics of the changes seen in arterial occlusion. In both cases, there were decreases in the concentration of the oxygenated hemoglobin fraction and increases in the concentration of the deoxygenated fraction.

At the same time, there were some characteristic features. The decrease in the concentration of the oxygenated hemoglobin fraction in the forearm tissues during arterial occlusion occurred more slowly than the decrease in the concentration of the oxygenated hemoglobin fraction in muscle tissue during exertion.

The data presented in Figs. 1c and 2c and f show that the rates of change in the concentration of the oxygenated hemoglobin fraction v_{decr}^{fo} , v_{decr}^{qe} , and v_{decr}^{be} were determined for forearm tissues in conditions of arterial occlusion and in muscle tissue during loading of the quadriceps femoris muscle and biceps brachii muscle, respectively:

$$v_{decr}^{fo} = 0.3 \text{ } \mu\text{mol/s};$$

$$v_{decr}^{qe} = 1.1 \text{ } \mu\text{mol/s};$$

$$v_{decr}^{be} = 3.5 \text{ } \mu\text{mol/s}.$$

Restoration of the concentration of the oxygenated hemoglobin fraction in the forearm tissues after occlusion ended was faster than in muscle tissue after completion of exertion:

$$v_{rec}^{fo} = 3.5 \text{ } \mu\text{mol/s};$$

$$v_{rec}^{qe} = 0.4 \text{ } \mu\text{mol/s};$$

$$v_{rec}^{be} = 2.2 \text{ } \mu\text{mol/s}.$$

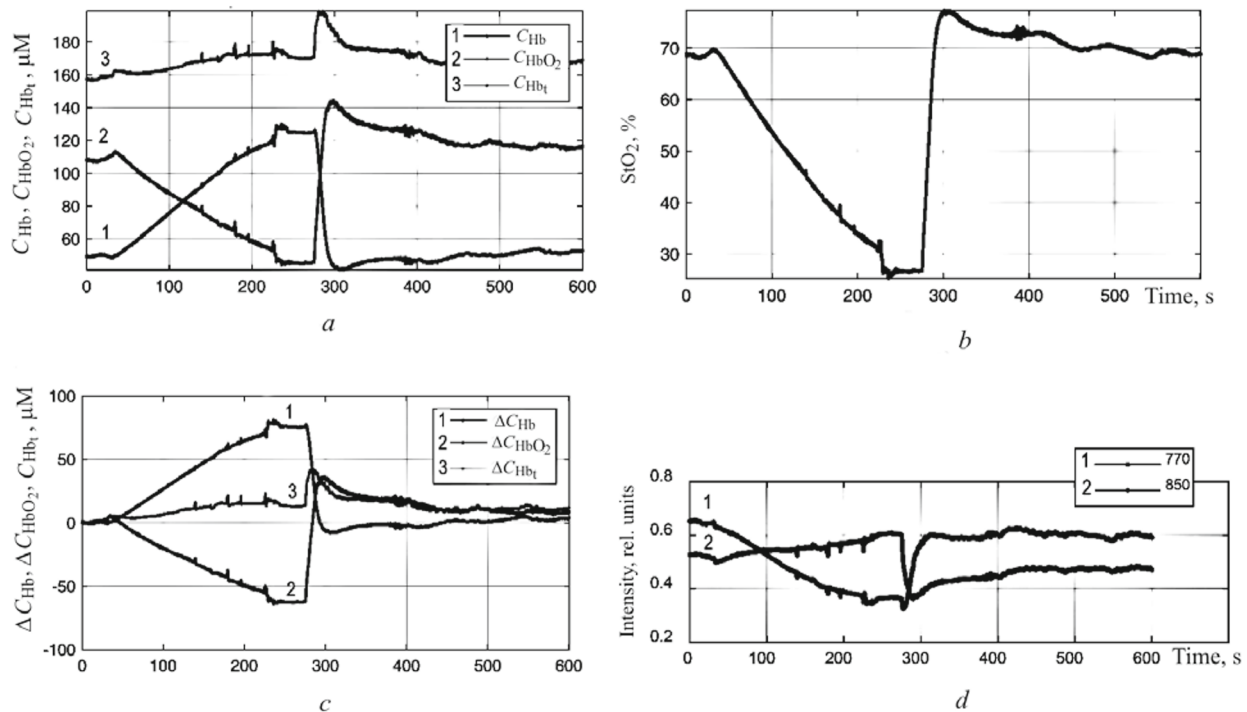


Fig. 1. Measurement of hemoglobin oxygenation parameters during arterial occlusion: a, b) absolute values of the concentrations of hemoglobin fractions and saturation values calculated using the present algorithm; c) relative values of the concentrations of hemoglobin fractions calculated using the present algorithm (changes relative to the state of rest); d) initial data obtained using the device.

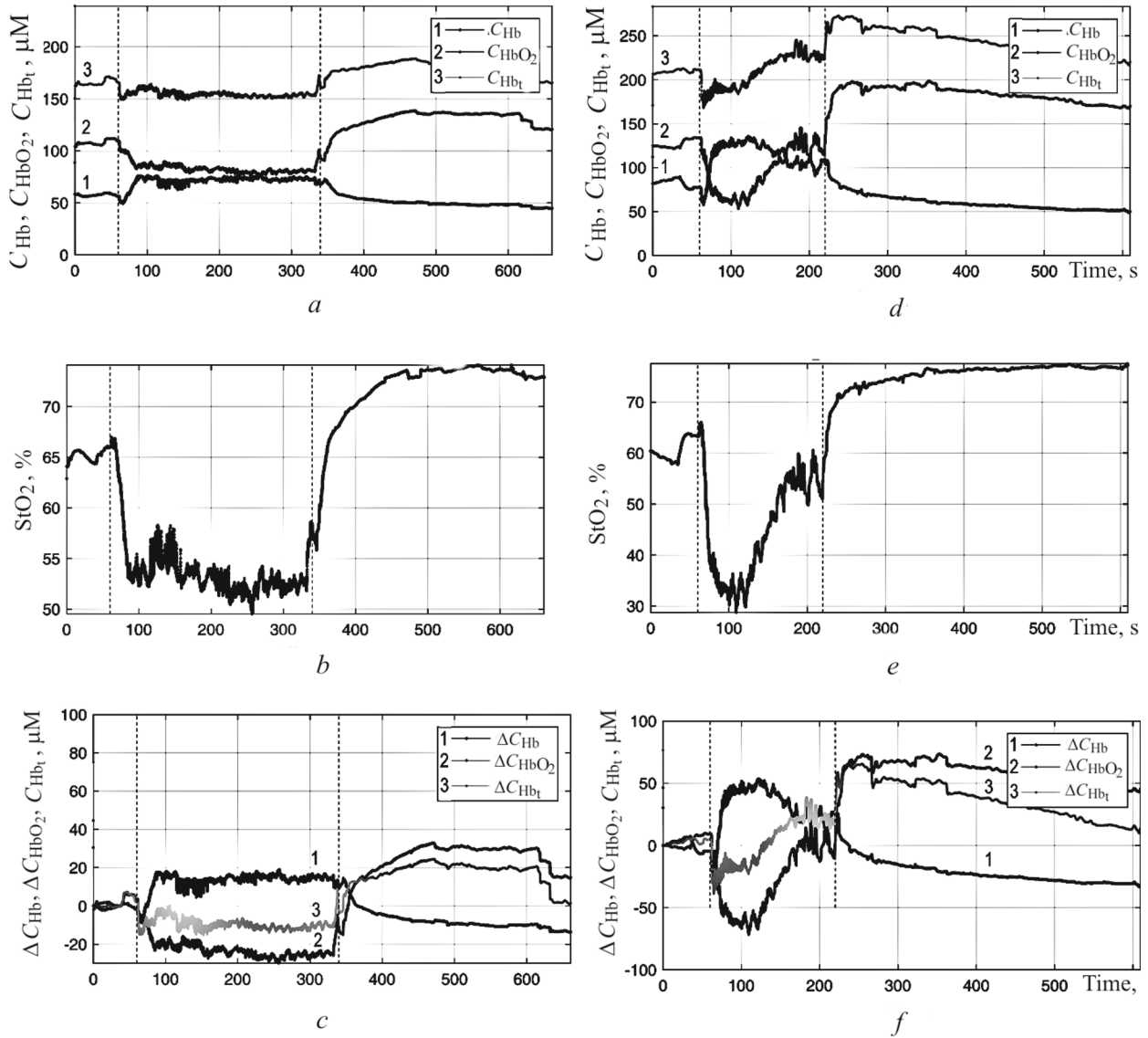


Fig. 2. Measurement of the hemoglobin oxygenation parameters during exertion of the quadriceps femoris muscle (a–c) and the biceps brachii muscle (d–f): a, b, d, e) absolute values of the concentrations of hemoglobin fractions and saturation values calculated using the present algorithm; c, f) relative concentrations of hemoglobin fractions calculated using the present algorithm (changes relative to the state of rest). The first vertical dashed line corresponds to the beginning of exertion, the second to the end.

Differences were seen in the dynamics of restoration of the concentration of the oxygenated hemoglobin fraction in the muscles. On exertion of the quadriceps femoris muscle, there was a gradual decrease during exertion and recovery began immediately after exertion ended (Fig. 2b), while the concentration of the oxygenated hemoglobin fraction on exertion of the biceps brachii muscle began to recover during exertion, almost immediately after the decrease in the concentration to the minimum value, and there was a

sharp increase in the recovery rate after exertion ended (Fig. 2e). This effect was probably associated with different types of hemodynamics in different muscles, as well as with differences in the nature of the exertion applied to the muscles: participants' subjective impressions were that muscle exertion was more intense in the second experiment.

The measurement method developed here yielded hemoglobin oxygenation and saturation values which were consistent with typical values obtained using other devices

and measurement methods known from the literature, showing that the NIRS4 system and the present algorithm can be used to analyze the dynamics of muscle oxygenation.

Conclusions

This report presents results from measurements of the absolute and relative concentrations of the oxygenated and deoxygenated hemoglobin fractions using the NIRS4 system and the present measurement algorithm. A number of experiments were run using the NIRS4 complex, and characteristic features of the dynamics of changes in hemoglobin oxygenation parameters during arterial occlusion and physical exertion of the quadriceps femoris and biceps brachii muscles were identified. These results demonstrate that the NIRS4 system, together with the present algorithm based on the modified Bouguer–Lambert–Beer law, can be used to analyze the dynamics of hemoglobin oxygenation.

This study was carried out within the framework of state contract of the Ministry of Education and Science of the Russian Federation (Agreement No. 075-03-2023-024 of January 13, 2023).

REFERENCES

1. Mesquida, J., Gruartmoner, G., and Espinal, C., "Skeletal muscle oxygen saturation (StO₂) measured by near-infrared spectroscopy in the critically ill patients," *BioMed. Res. Int.*, **2013**, Article ID 502194 (2013).
2. Yang, Y., Soyemi, O. O., Scott, P. J., Landry, M. R., Lee, S. M., Stroud, L., and Soller, B. R., "Quantitative measurement of muscle oxygen saturation without influence from skin and fat using continuous-wave near infrared spectroscopy," *Optics Express*, **15**, No. 21, 13,715–13,730 (2007).
3. Ferrari, M., Mottola, L., and Quaresima, V., "Principles, techniques, and limitations of near infrared spectroscopy," *Can. J. Appl. Physiol.*, **29**, No. 4, 463–487 (2004).
4. Tuchin, V. V., "Optics of biological tissues," in: *Light Scattering Methods in Medical Diagnostics* [in Russian], Fizmatlit, Moscow (2012).
5. Buyanov, D. A., Shalaev, P. V., Zabodaev, S. V., Gerasimenko, A. Yu., "An algorithm for measuring absolute and relative hemoglobin concentrations using near infrared spectroscopy," *Biomed. Eng.*, **56**, No. 3, 176–179 (2022).
6. Rogatkin, D. A., "The physical basis of optical oxymetry," *Meditinsk. Fizika*, No. 2, 97–114 (2012).
7. Rolfe, P., "In vivo near-infrared spectroscopy," *Ann. Rev. Biomed. Eng.*, **2**, No. 1, 715–754 (2000).
8. Colier, W., *Near Infrared Spectroscopy: Toy or Tool? An Investigation on the Clinical Applicability of Near Infrared Spectroscopy*, Katholieke Universiteit Nijmegen, 105 (1995).
9. Jones, B., Dat, M., and Cooper, C. E., "Underwater near-infrared spectroscopy measurements of muscle oxygenation: Laboratory validation and preliminary observations in swimmers and triathletes," *J. Biomed. Opt.*, **19**, No. 12, Article ID 127002 (2014).
10. Fantini, S., Hueber, D., Franceschini, M. A., Gratton, E., Rosenfeld, W., Stubblefield, P. G., Maulik, D., and Stankovic, M. R., "Non-invasive optical monitoring of the newborn piglet brain using continuous-wave and frequency-domain spectroscopy," *Phys. Med. Biol.*, **44**, No. 6, 1543–1563 (1999).
11. Ferrari, M., Binzoni, T., and Quaresima, V., "Oxidative metabolism in muscle," *Phil. Trans. Roy. Soc. Lond. B Biol. Sci.*, **352**, No. 1354, 677–683 (1997).